



## Emulsification in novel ultrasonic cavitation intensifying bag reactors



Ralph van Zwieten<sup>a</sup>, Bram Verhaagen<sup>b</sup>, Karin Schroën<sup>a,\*</sup>, David Fernández Rivas<sup>b,c,\*</sup>

<sup>a</sup> Food Process Engineering Group, Wageningen University, 6700AA Wageningen, The Netherlands

<sup>b</sup> BuBclean, 7622PH Borne, The Netherlands

<sup>c</sup> Mesoscale Chemical Systems Group, University of Twente, 7500AE Enschede, The Netherlands

### ARTICLE INFO

#### Article history:

Received 18 July 2016

Received in revised form 20 November 2016

Accepted 2 December 2016

Available online 19 December 2016

#### Keywords:

Ultrasound

Emulsification

Process intensification

Process chemistry

Cavitation

Sonochemistry

### ABSTRACT

Cavitation Intensifying Bags (CIBs), a novel reactor type for use with ultrasound, have been recently proposed as a scaled-up microreactor with increased energy efficiencies. We now report on the use of the CIBs for the preparation of emulsions out of hexadecane and an SDS aqueous solution. The CIBs have been designed in such a way that cavitation effects created by the ultrasound are increased. It was found that the CIBs were 60 times more effective in breaking up droplets than conventional bags, therewith showing a proof of principle for the CIBs for the preparation of emulsions. Droplets of 0.2  $\mu\text{m}$  could easily be obtained. To our knowledge, no other technology results in the same droplet size more easily in terms of energy usage. Without depending on the wettability changes of the membrane, the CIBs score similarly as membrane emulsification, which is the most energy friendly emulsification method known in literature. Out of the frequencies used, 37 kHz was found to require the lowest treatment time. The treatment time decreased at higher temperatures. While the energy usage in the current non-optimised experiments was on the order of  $10^7 - 10^9 \text{ J/m}^3$ , which is comparable to that of a high-pressure homogenizer, we expect that the use of CIBs for the preparation of fine emulsions can still be improved considerably. The process presented can be applied for other uses such as water treatment, synthesis of nanomaterials and food processing.

© 2016 Elsevier B.V. All rights reserved.

### 1. Introduction

The use of ultrasonic waves has been considered as a simple, inexpensive, and valuable tool in chemistry because of its “green” character while promoting faster and selective transformations [1]. Scalability, high safety, low waste generation, and energy efficiency are also important qualities of a process for its successful commercialisation and adoption by industry. [2,3] The advantages of using ultrasound for industrial chemical engineering processes have been described for processes such as defoaming, emulsification, extraction, and drying, as well as for environmental applications such as water remediation, pharmaceuticals, cosmetics and in food processing [4–10]. Following the concept of Process Intensification as a tool to achieve more sustainable and efficient chemical engineering processes [11], ultrasound has been used extensively, alone and in combination with other activation techniques such as microwaves, with significant improvement of process efficiency, together with waste and energy consumption reduction [1,12–15].

The use of ultrasound for the creation of emulsions is based to a great extent on the process of cavitation. The ultrasound is generated by a piezoelectric actuator resulting in pressure fluctuations, leading to the formation and activation of bubbles in the liquid (cavitation). The oscillation and collapse of these bubbles lead to large velocities ( $\sim 100 \text{ m/s}$ ) on small scales ( $\sim 10 \mu\text{m}$ ), which is very useful for local mixing to make droplets, and other associated physicochemical phenomena of practical uses known as sonochemistry [16,17].

Emulsions are dispersions of two (or more) immiscible liquids, and are widely used in various industries including food, cosmetics, pharmaceuticals, paints, asphalt, etc. [18,19]. Several devices can be used to make an emulsion, amongst which high-pressure homogenizers, rotor–stator systems and ultrasound treatment are the prevailing methods. Recently, microfluidic devices are receiving more attention because they allow better control over the micrometer scale: the scale that is important in the structuring of foods [20]. Control relates to both the droplet size and monodispersity of the emulsion that can be obtained, unlike classic techniques that make rather polydisperse emulsions. Emulsions having a droplet span lower than 0.4 are considered to be monodisperse [21]. Microstructured emulsification devices are also known for their relatively low energy demand, which is an important rea-

\* Corresponding authors at: Mesoscale Chemical Systems Group, University of Twente, 7500AE Enschede, The Netherlands (D. Fernández Rivas).

E-mail addresses: [karin.schroen@wur.nl](mailto:karin.schroen@wur.nl) (K. Schroën), [d.fernandezrivas@utwente.nl](mailto:d.fernandezrivas@utwente.nl) (D. Fernández Rivas).

son for the increasing interest in their use in industry. Some of the main micro-emulsification techniques include the T-shaped junction, flow focusing devices, the EDGE method, and membrane emulsification [22].

It is known that the physical stability of emulsions increases when the size of the droplets in the dispersed phase becomes smaller, the viscosity of the continuous phase is higher, and the density ratio between both phases is minimal [23]. In 1851 Sir George G. Stokes derived the following equation for a single droplet present in a large amount of continuous phase [24]:

$$v = \frac{g(\rho_c - \rho_d)2R_d^2}{9\eta} \quad (1)$$

In which  $v$  is the creaming or sedimentation velocity in m/s;  $(\rho_c - \rho_d)$  the density difference between the continuous and dispersed phase in kg/m<sup>3</sup>;  $R_d$  the droplet radius in m; and  $\eta$  the viscosity of the continuous phase in Pa·s. However, making small droplets involves increasing the surface area of the droplets, thereby increasing the Gibbs free energy. To this aim, a considerable amount of energy is needed  $\sim 10^8$  J/m<sup>3</sup>, which in practice is much more than the minimal amount of energy necessary to create the interfacial area. This happens because interfaces are not duly stabilized, leading to coalescence and energy is dissipated as heat during preparation [23].

One drawback of common ultrasonic systems is that they require significant amounts of energy in order to generate sufficient bubbles for emulsification, which is partly due to the fact that the generation of bubbles is a nearly stochastic process and difficult to control [25]. The energy applied by ultrasound cannot be used as efficiently as in the high pressure homogenization device. A first possible explanation is that a broad distribution of shear rates may be created in the ultrasound unit, providing shear rates not always sufficient to break up the droplets. Another possibility is related to the residence time of the droplets in the shear zone being too short to deform and disrupt droplets [26]. The presence of bubbles in the liquid can additionally negatively influence energy transmission since they scatter sound, shielding certain regions in the liquid [25]. In general, this technique is applied to specific emulsion formulations, e.g. those that do not contain vegetable oils that might suffer oxidation of the product as a result of radicals produced by ultrasonic cavitation [27].

The synergy of sonochemistry and microfluidics has been praised as a greener technology [15,28–30], demonstrating its advantages for chemical synthesis, crystallization, and solid forming reactions [31–33], etc. The chemical initiation on emulsion polymerisations, exfoliation and synthesis has been demonstrated, having better conversion results when combined with ultrasound, and in certain cases without additives nor conventional methods [34–38].

The effect of ultrasound is known to be localised when used for emulsification; the liquids need to be brought closely to the position where the effects of cavitation are largest [23]. In standard ultrasound equipment, the cavitation is not controlled, meaning it can take place at various locations inside the sonicated volume of liquid, leading to suboptimal processing. For example, hot spots and pressure (anti) nodes are present in the liquid volume of an ultrasonic bath, meaning that there are sections that have almost no cavitation.

Here we present our solution for controlling cavitation through the use of a novel device known as the Cavitation Intensifying Bag (CIB) (commercialised as BuBble bags by BuBclean, Enschede, The Netherlands); which is a scaled-up microfluidic sono-reactor [39]. It was originally developed for cleaning purposes, but it also gave improved radical formation and reproducibility of results [40]. In this work we present results of this technology used for

emulsification. The CIB can be seen as an intensified batch reactor, with scaling up potential and the possibility of converting it into a continuous flow reactor concept.

The CIBs are plastic bags that are modified to include pits (indentations) in their inner surfaces. There are ca. 900 pits inside the CIBs, with a spacing of 3.5 mm. The pits have a diameter between 100 and 500  $\mu\text{m}$  and a depth of 100–200  $\mu\text{m}$ ; more details can be found elsewhere [40]. When a liquid is poured inside (e.g. water, ethanol, acetone, surfactant solutions), a gas bubble can be trapped in the pits, depending on the gas content of the liquid. Upon exposure to ultrasound, microbubbles are generated in large quantities from these gas-filled pits. Earlier research showed that these CIBs are indeed able to enhance cavitation (radical formation and mechanical effects) [40]. The CIBs demonstrated to lead to a reduction of cleaning times with 86%, as well as 22% more reproducible and 45% more efficient generation of cavitation-related effects, such as emulsification [41]. To the best of our knowledge this is the first detailed investigation in which CIBs are used to produce emulsions under different experimental conditions.

In the current paper, we report on the various process parameters influencing the emulsification process of hexadecane and SDS solutions using CIBs. Amongst others, a comparison will be made between the CIBs and other emulsification methods with regard to monodispersity of the obtained emulsions, energy usage, and ease of upscaling. Furthermore, decentralised production of emulsions is discussed as a point that could favour application of CIBs in industrial settings.

## 2. Materials and methods

Emulsions of hexadecane ( $\text{C}_{16}\text{H}_{34}$ , ReagentPlus, 99%, Sigma-Aldrich) in water were prepared at concentrations of 5, 10, 15, 20 and 25% (volume/volume, v/v) by adding hexadecane to a CIB that was first filled with a 1% SDS (ACS reagent, >99%) aqueous solution (Milli-Q system ZMQS 50001, Millipore). The total volume in the

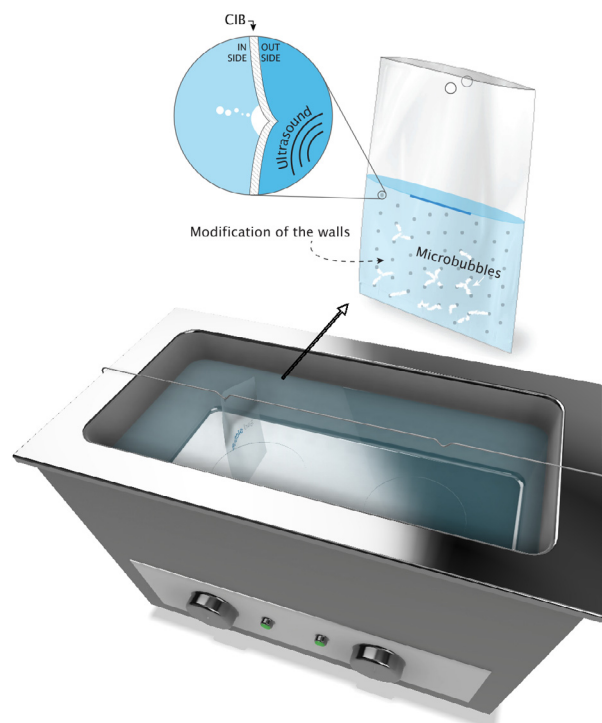


Fig. 1. Overview of the setup. The CIB (top) is positioned inside an ultrasonic bath (bottom) above one of its transducers.

bag was between 11 and 15 ml. The CIB containing the two unmixed liquids was placed inside an ultrasonic bath (P60H, Elma, Singen, Germany; sweep and pulse off), directly above one of the transducers of the ultrasonic bath using a custom-made hanging rod (see Fig. 1). The frequencies used were 37 and 80 kHz and the amplitude was set to 100%. The bath was filled with 1/3 tap water and 2/3 demi water at 21 °C. In most experiments the water remained at room temperature, but some were carried out with the water heated to 80 °C (and at 37 kHz). The total ultrasonic treatment times varied from 30 min for a frequency of 37 kHz to 120 min for a frequency of 80 kHz, depending on the effectiveness of the emulsification process. The CIB treatment was compared to a conventional plastic bag (Minigrip, Lelystad, The Netherlands) with identical size but no pits on its inner surface, using a 15% hexadecane concentration.

The resulting emulsion droplet size distribution and the average droplet diameter  $d_{32}$  were measured after various time intervals using a dynamic light scattering particle size counter (Mastersizer Hydro 2000 SM, Malvern, Worcestershire, UK). These physical parameters were only determined when a fully dispersed emulsion was obtained (determined by eye) and the phases were completely mixed. If this was not yet the case, the CIB was put back into the bath and the process was resumed. In case a fully dispersed emulsion was observed, the process was paused and a sample of ca. 1 ml was taken using a transfer pipette. Single experiments were carried out, the results of which are shown in the next section.

### 3. Results and discussion

#### 3.1. CIBs vs. conventional bags

First, emulsions obtained with CIBs are compared with that of regular bags. To illustrate the difference, Fig. 2 shows the droplet size distribution in 15% v/v hexadecane in water emulsions containing 1% (w/v water) SDS for both types of bags that were exposed to 37 kHz. It is clear from Fig. 2a that the droplet size produced in a CIB after 15 min is considerably smaller than that in a conventional bag after the same exposure time. The largest droplet size obtained with the unmodified bag is about 30  $\mu\text{m}$  whereas no droplet was larger than approximately 9  $\mu\text{m}$  for the CIB. The average volume of the droplets decreased with a factor of 60 (based on  $d_{32}$ ), which clearly demonstrates that the CIBs facilitate droplet formation, presumably enhanced by cavitation effects. The bubbles that are formed by cavitation perform rapid oscillation and collapse along the water/oil interface, which disrupts this interface resulting in the emulsion being formed [42]. When plotted on a logarithmic scale, as shown in Fig. 2b, it is easier to observe how many small droplets are formed especially when using the CIB.

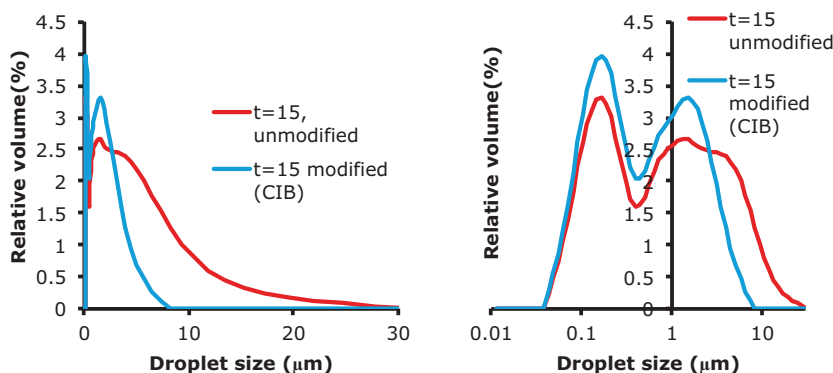


Fig. 2. The droplet size distribution of hexadecane in water emulsions (15%, 1% SDS). The emulsions were prepared at 37 kHz and 20 °C. The data are shown on a linear (left) and logarithmic scale (right).

This also implies that stability against creaming has been increased considerably as can be deduced from Stokes law (Eq. (1)). Many droplets are well below 1  $\mu\text{m}$ , which also positions the CIB process in the lower regions of Fig. 8, as will be discussed further in this section.

From Fig. 2 it is clear that the CIB enhances emulsification; the effect of various processing parameters, such as processing time, oil volume fraction, frequency, and temperature, is discussed in the next sections.

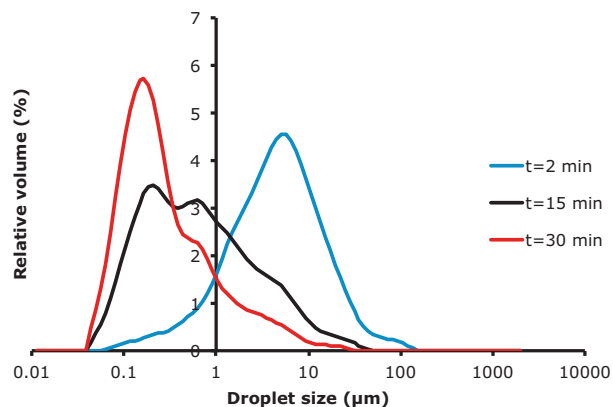
#### 3.2. Processing time

Fig. 3 shows the resulting droplet size distribution at three different ultrasound treatment times: 2, 15, and 30 min; the emulsion contained 5% hexadecane and 1% SDS, and emulsification is carried out at 80 kHz. In this experiment, the oil was incorporated in the emulsion after 2 min treatment. At 2 min treatment, the largest droplets were about 100  $\mu\text{m}$ , which are split up into much smaller ones at higher treatment times. The droplet size decreased considerably at higher treatment times. As is the case in standard emulsification processes, the local energy needs to be such that larger droplets break up into smaller ones. This occurs in consecutive steps (not in one step), until the local energy is no longer high enough to break up the droplets that are continuously decreasing in size. Similar graphs were obtained at a frequency of 37 kHz.

#### 3.3. Oil volume fraction

In Fig. 4, the droplet size is plotted as a function of treatment time for various oil fractions at 1% SDS concentration. All samples were treated at 80 kHz. From Fig. 4 it is clear that more time is needed to emulsify higher oil concentrations and to reach similar droplet size.

For all concentrations and at 80 kHz, small droplets in the sub-micrometer range that are very stable against creaming were obtained (see equ. 1). The average droplet size decreased even further when applying longer treatment times. In Fig. 4, the 5% and 10% graphs show a fast reduction in droplet size, and the two highest oil concentrations decrease their size the slowest. Since the applied energy is used (at least partly) to break up droplets, it is expected that emulsions with lower oil volume fractions would reach smaller sizes faster. The time at which e.g. a size of 0.4  $\mu\text{m}$  is reached does not necessarily scale with the volume fraction that is used (Fig. 4), and this may be due to effects that attenuate the ultrasound. The formed droplets might form barriers for the ultrasound to protrude the solution and reduce the effectiveness of droplet formation. But also other aspects can play a role: upon increasing the hexadecane fraction in the emulsion, the frac-



**Fig. 3.** Droplet size distribution at three different ultrasound treatment times (2, 15 and 30 min) inside the CIB at 80 kHz and 20 °C.

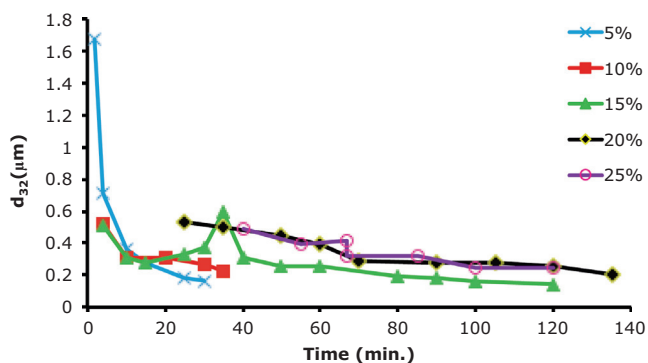


**Fig. 4.** The average droplet size ( $d_{32}$ ) as function of time at 80 kHz and 20 °C for five different concentrations of hexadecane (5, 10, 15, 20 and 25%). The peak in the line for an oil fraction of 15% might be due to non-ideal mixing within the CIB.

tion of water in which cavitation takes place will decrease, leading to less cavitation per unit volume of hexadecane. Besides, when hexadecane is incorporated into the continuous water phase, the viscosity of the emulsion is higher, the acoustic modulus of the liquid is changed and thus the ultrasound may reach the inside of the CIB weakened, leading to milder bubble collapses. Also, because the oil layer first lies on top of the water/sds layer, it takes time before the entire body of oil is processed into the water phase. Therefore a larger droplet may initially be present that requires time to be turned into smaller droplets. The thicker this oil layer, the more energy needed in the system before a particular droplet size is obtained.

### 3.4. Frequency

An experiment similar to the one described in the previous section was also carried out at 37 kHz, with the results shown in Fig. 5. It is clear that also at this lower frequency very small droplets can be made, and that the rate at which droplet size reduction takes place is a function of the oil volume fraction (see Fig. 4). At the lowest concentration, the emulsion established at shorter times than at higher concentrations, and these droplets were relatively large, when compared to the first points taken at higher concentration. If the first points were all taken after 2 min, we expect that the diameter for the 5% emulsion would be in line with the values found for 10 and 15%, because the initial size reduction takes place much more rapidly than for longer treatment times, simply because the smaller the droplets are, the more difficult their size can be reduced (see also arguments elsewhere in this text). How-

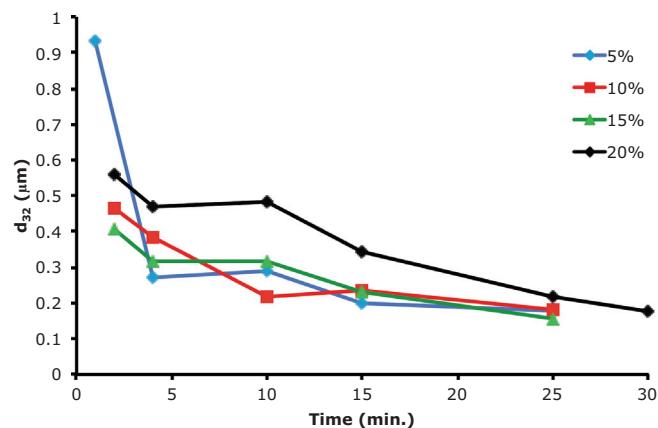


**Fig. 5.** The average droplet size ( $d_{32}$ ) as function of time at a frequency of 37 kHz for four different concentrations of hexadecane (5, 10, 15 and 20%).

ever, the reduction in droplet size is faster at low energy input, as is illustrated in Fig. 6 for selected experiments, which could be an evidence that inertial (or mechanical) effects of cavitation are influencing the break-up of droplets [43].

Fig. 6 shows that the data for the lowest concentration of hexadecane (5%) at the highest frequency (80 kHz) follows a similar trend with those for the higher concentrations (15 and 20%) at the lowest frequency (37 kHz). This effect is even clearer when comparing only the 20% hexadecane samples at different frequencies. At a frequency of 80 kHz, a fully dispersed emulsion was not yet obtained until  $t = 25$  min, while at a frequency of 37 kHz a proper emulsion was already visible at  $t = 2$  (15%), respectively at  $t = 4$  min (20%).

In addition, when considering the 20% concentration data, the graph for 80 kHz lies entirely above the graph for the lower frequency. This effect was also mentioned in literature [44]; for the same cavitation effects, more power is required at higher frequencies. At low frequency, where a long acoustic cycle exists, large bubbles are created. At high frequency, the acoustic cycle is short and therefore the bubbles are smaller. This results in a less violent cavitation collapse, with milder mechanical effects, and thus a lower droplet formation rate; this in turn leads to a longer processing time. This is elaborated on in the appendix in which the process time is also related to the amount of oil that needs to be emulsified. At 80 kHz, the process efficiency is a function of the oil fraction, while at 37 kHz this effect is less pronounced. Apparently, the ultrasound waves created at 37 kHz hold more energy which results in a higher shear force, while the ultrasound at 80 kHz hold less energy and less penetration depth. Though not verified for

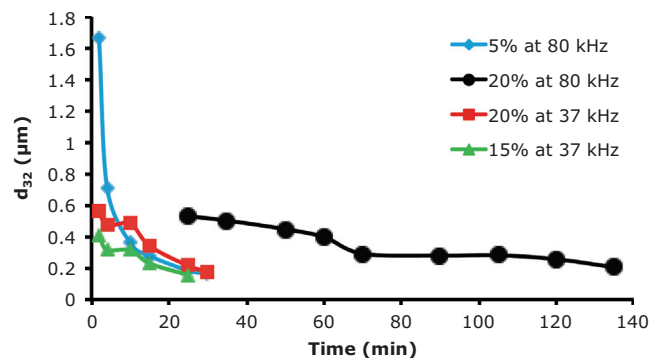


**Fig. 6.** A comparison of the average droplet size ( $d_{32}$ ) as function of time at different frequencies (37 and 80 kHz) and at different concentrations of hexadecane.

these particular experiments, shielding effects are more noticeable at higher frequencies [25,45].

From the perspective of economically sustainable processing, the amount of energy needed to obtain the desired droplet size is important. Since the electrical power is almost the same for both frequencies (680 and 640 W for 37 and 80 kHz respectively), it is in this respect crucial to keep the processing time as short as possible while creating the same average droplet size, and for this clearly the lower frequency is preferred. For e.g. a droplet size of 0.2  $\mu\text{m}$ , 30 min are needed at 37 kHz, while at 80 kHz this takes 130 min, and this is directly coupled to the energy usage. Besides the lower frequency leads to less attenuation of ultrasound and less heating, which is an additional reason to prefer the low frequency of 37 kHz [25,44].

### 3.5. Viscosity and temperature

As mentioned before, viscosity may influence the efficacy of the ultrasound treatment; therefore we compared emulsification at 20 and 80 °C. Fig. 7 shows the droplet size distribution after 15 and 25 min at 37 kHz, 15 v/v% oil, and 1% SDS. At both temperatures, the droplet size reduces considerably, and small droplets were obtained. This effect was stronger at higher temperature. The lower viscosity changes the bubble dynamics (maximum radius, pressure reached during collapse, etc.), and a lower intensity and energy is needed to induce cavitation. Additionally, the interfacial tension is lower, and this facilitates droplet formation [44]. On the other hand, the vapor pressure of the solvent is higher at higher temperatures, and this leads to less violent collapse of the bubble; this may counteract the previously mentioned effects. However, at 80 °C the latter effect does not seem to outweigh the more powerful cavitation effects that were mentioned earlier. Experiments performed at the same temperature and at a frequency of 80 kHz resulted into the liquids leaking out of the bags. This might be due to increased erosion processes at these conditions [40], or the sealed edges of the CIB might loose its tightness.

### 3.6. Comparing emulsification with microstructured devices to CIBs

A comparison of several microstructured emulsification techniques [20] is reproduced in Table 1, where ultrasonic emulsification using CIBs is added as well. The monodispersity of the CIB technique is rather average, and the energy input is rather high. The CIB technique does allow preparation of larger amounts of emulsions than the other microfluidic techniques, and it could be scaled-up further. These amounts are such that properties (e.g.

rheological) of the emulsion can be determined, which is not possible when using the other microfluidic techniques. This latter aspect is in our view the most promising aspect of CIBs: to use them only an ultrasonic bath is required, and emulsions with very small droplet sizes can be prepared within minutes, i.e. on demand. Although CIBs behave similarly as membrane emulsification regarding the amount of product that can be made (Table 1), the latter process is sensitive to wettability changes of the membrane. This requires the ingredient and processing conditions to be chosen very carefully [46]. This is a great advantage in the use of ultrasound in combination with the CIBs. In addition, although the droplet size obtained by the various techniques is not shown in Table 1, this is also a very positive aspect of the use of CIBs in combination with ultrasound, as shown in Fig. 8. A droplet size of 0.2  $\mu\text{m}$  is very low compared to other emulsification techniques.

### 3.7. Energy considerations

As mentioned previously, the energy usage of emulsification techniques in relation to the droplet sizes created is a very important parameter for comparing among them. For microfluidic devices it is known that the required energy input is much lower than the classic techniques such as high pressure homogenization due to the lower applied pressure [20], see also Fig. 8. It has to be noted that these devices have not been tested yet for small droplet sizes. The only technique that is proven to be capable of making small droplets at low energy density is cross-flow membrane emulsification [47].

Not taken into account in Fig. 8 are the monodispersity of the droplets, and the scalability of some of the techniques. For the shear-based microfluidic devices it should be mentioned that their scalability has not been proven yet; often when scaling up through parallelization, the units interact, which leads to preferential flow towards some of the pores. This causes the droplets to become polydisperse or to be very difficult to control [54,55]. This drawback is not reported for spontaneous emulsification techniques such as straight-through microchannels and EDGE devices.

The energy efficiency when using the CIB for the different oil fractions used is estimated from the time for a certain value of  $d_{32}$  to be obtained. This time in minutes was then multiplied by the power required for each frequency (680 and 640 W for 37 and 80 kHz respectively). By taking into account the amount of oil and by assuming a total volume of 1.5 L of emulsion being prepared, the energy usage as shown in Fig. 9 was obtained.

From the results shown in Fig. 9, we can interpret that at very low oil concentration, the bubbles that are generated are not all close enough to oil droplets to generate smaller droplets, and energy is wasted. At higher concentrations (10–15%), it seems that the ratio between droplet size and bubble size is rather optimal for generation of droplet break-up, while at even higher oil fractions more energy is needed. This is partly because more oil needs to be broken up into small droplets, and besides the presence of so many droplets will make the efficiency of the ultrasound less effective due to the previously described viscosity effects. How larger the droplets, how easier to break up. The interfacial tension force scales with  $1/r$  which makes small droplets much less deformable, and that is needed for break-up. That is not only the case for the CIBs, but for any emulsification device.

At a frequency of 80 kHz and 15% of oil, an approximation was made for the energy usage because of the peak shown in Fig. 4. Also, no data were available on the energy usage at this frequency and at a  $d_{32}$  of 0.2 at the highest oil volume fraction, since this size was not found. At 37 kHz no data were available for a  $d_{32}$  of 0.5 because the size of the droplets was already smaller at the first measurement.

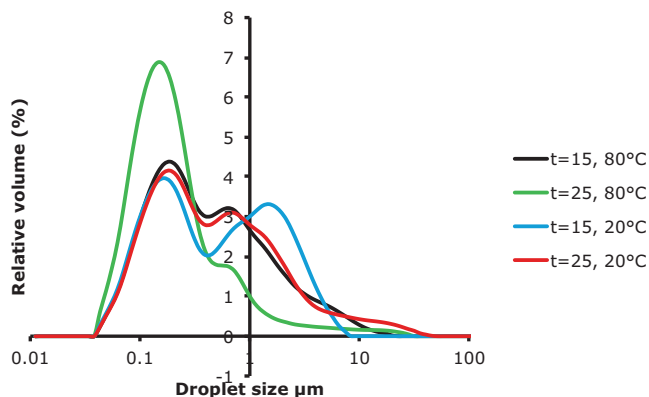


Fig. 7. The droplet size distribution for emulsification at 20 and 80 °C, a processing time of 15 or 25 min. All four graphs are measured at a frequency of 37 kHz and a concentration of 15% hexadecane.

**Table 1**  
Comparison of microstructured emulsification techniques.

| Emulsification technique            | Phase to be controlled <sup>a</sup> | Mono-dispersity <sup>a</sup> | Amount of product <sup>b</sup> | Energy input <sup>a,b</sup> | Droplet size range ( $\mu\text{m}$ ) |
|-------------------------------------|-------------------------------------|------------------------------|--------------------------------|-----------------------------|--------------------------------------|
| T-junction                          | Continuous & dispersed              | ++                           | --                             | --                          | $10^0 - 10^1$                        |
| Flow focusing                       | Continuous & dispersed              | ++                           | --                             | --                          | $10^{-1} - 10^0$                     |
| $\mu$ channel/straight through/EDGE | To be dispersed                     | +++                          | -                              | +                           | $10^1 - 10^2$                        |
| Membrane (direct)                   | Continuous & dispersed              | o                            | o                              | o                           | $10^{-1} - 10^1$                     |
| Membrane (pre-mix)                  | Pre-mix                             | -                            | o                              | -                           | $10^0 - 10^1$                        |
| Ultrasonic using CIB's              | None                                | o                            | o                              | --                          | $10^{-1} - 10^0$                     |

+ or – means scores better or worse than the standard technology (direct membrane emulsification).

<sup>a</sup> Direct membrane emulsification is the benchmark, and denoted with a neutral value (o).

<sup>b</sup> Assuming equal channel dimensions for the microfluidic devices.

\* Feed liquids that need to be controlled in order to make ‘monodisperse’ droplets.

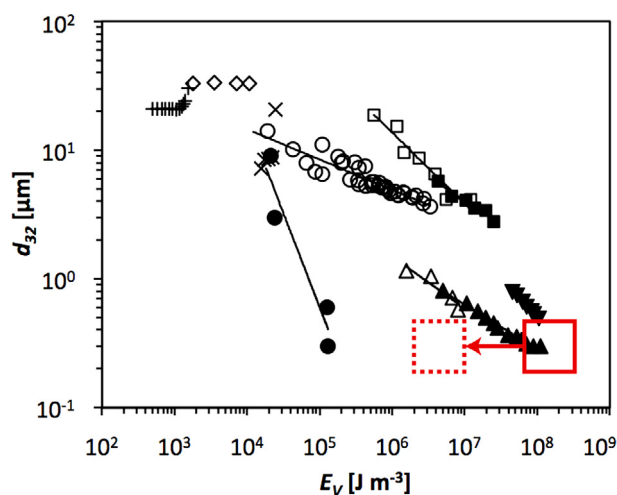


**Fig. 8.** Comparison of energy density of different emulsification techniques. The  $d_{32}$  is shown as a function of energy density,  $E_V$ , for various emulsification devices: (+) grooved microchannel [48], ( $\diamond$ ) straight-through microchannel [49,50], ( $\times$ ) EDGE emulsification [51], ( $\square$ ) Y-junction [52], ( $\circ$ ) premix emulsification using  $55 \mu\text{m}$  glass beads, ( $\bullet$ ) cross-flow membrane emulsification [53] ( $\blacksquare$ ) flat valve homogenizer [53], ( $\triangle$ ) orifice valve [53], ( $\blacktriangle$ ) microfluidizer [53], and standard ultrasonic homogenizers ( $\blacktriangledown$ ) [47]. The solid red rectangle shows the values estimated from the present study; the dashed rectangle shows projected values assuming 100-fold increase in emulsification efficiency (adapted from [47]).

From the above, it is clear that more energy is needed to obtain small droplets, when just focusing on one frequency. When comparing 37 and 80 kHz, the process efficiency is much higher for a frequency of 37 kHz (much lower energy usage per volume of oil). This is caused by the previously discussed effect of the formation of larger bubbles at 37 kHz that collapse much more violently, and that do not or much less experience shielding from the droplets that are present in the emulsion.

When comparing with the data in Fig. 8, the CIB would be in the lowest part of the graph in regard to droplet size and in the same

range as the high pressure homogenizers in terms of energy usage. This is indicated by the rectangle in Fig. 8. The lower frequency, being much more effective than the higher frequency, is in the left part of this rectangle. The process with CIBs as carried out in this study is expected to be far from optimal. From improved positioning of the ultrasound transducer relative to the cavitation bag, as well as larger volumes of emulsion compared to the amount of water in the bath, the efficiency of the process can be improved by at least a factor of 10 but possibly with a factor of 100 (dashed rectangle in Fig. 8). This would need to be the result of a purpose-built bath that operates over short length scales.

As mentioned, CIBs can produce small droplets in a reproducible way, which makes them interesting devices for the production of emulsions on larger scale and higher throughputs. The current set-up allows the preparation of samples of 10–20 ml, but clearly that is not the limit. Large volumes are processed regularly in industrial applications compared to the small size of the CIBs and the ultrasonic baths used in this research and that are common in laboratories. When using larger bags, larger amounts of emulsions can be made as long as the cavitation sites are in close proximity of the liquids (interfaces) that need to be emulsified. How the dimensions of the bags and the ultrasound bath can be matched in the best possible way is part of follow-up research.

#### 4. Conclusions

The proof of principle that emulsification with ultrasound can be enhanced by the use of specific surface modifications in bags is given in this paper, alongside the effect of various process parameters that can be used to modulate the droplet size. The process is more energy efficient at a frequency of 37 kHz than at 80 kHz. Increasing the temperature of the liquid leads to a decrease in required processing time, but also consumes more (electrical) energy, and is only suited for the lower frequency.

When comparing different techniques, we found that the CIB ultrasound technique stands out with regard to the small droplets produced, as well as the flexibility in using different emulsion com-

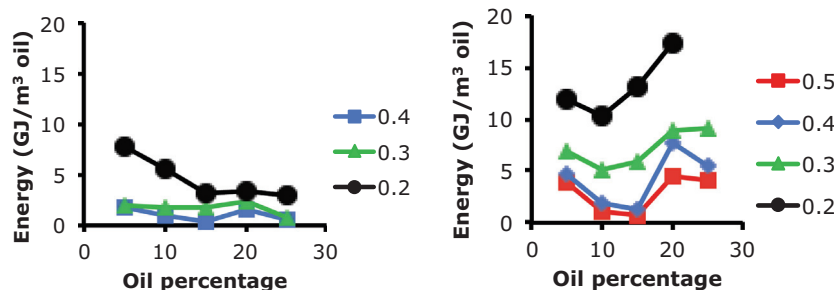


**Fig. 9.** Energy usage needed to obtain  $d_{32}$  of 0.5–0.2 vs oil fraction at 37 kHz (left) and 80 kHz (right). Values are given in GJ.

position. Based on the fact that a large number of laboratories have ultrasonic baths, the technique as it is right now is very accessible and suited to make smaller amounts of stable emulsions on demand.

There is no physical or practical limitation for the scalability of this concept: bags can be made bigger, a larger number of pits can be accommodated per unit area, and industrial scale ultrasonic reactors can be designed for an optimal utilisation of the diffuse acoustic energy. Nevertheless, there is an engineering challenge to be tackled as larger bags are used with cavitation activity happening only close to the walls of the bags, and not in the bulk liquid. Similarly, in our previous studies we have reported on the negative influence of interacting clusters of bubbles leading to lower energy efficiencies, and the erosion of the reactor walls; hence the density of pits cannot be increased infinitely. Clearly, the optimal configuration for a commercially appealing CIBs and its industrial adoption needs more investigation.

The same concept of the CIBs is of relevance to other important chemical processing and engineering applications, like in waste water treatment, where the generation of radicals is required to remove recalcitrant water contaminants. Similarly, in applications where the mechanical effects of ultrasound are more desired than the radical formation, the possibility of using shorter processing times with sufficient reproducibility can solve several limitations of ultrasonic processing, such as stringent requirements in food processing and nanomaterials synthesis. Further work is required to test an equivalent concept for continuous flow CIBs, as well as finding an optimal configuration in the spacing of the pits, which will be our next point of attention.

## Acknowledgements

We thank Jos Sewalt for technical assistance in the experimental work.

## References

- [1] G. Cravotto, P. Cintas, The combined use of microwaves and ultrasound: Improved tools in process chemistry and organic synthesis, *Chem. A: Eur. J.* (2007) 1902–1909, Cited By 38.
- [2] S.G. Newman, K.F. Jensen, The role of flow in green chemistry and engineering, *Green Chem.* 15 (6) (2013) 1456–1472.
- [3] A. Patist, D. Bates, Ultrasonic innovations in the food industry: From the laboratory to commercial production, *Innovative Food Sci. Emerg. Technol.* 9 (2) (2008) 147–154, *Food Innovation: Emerging Science, Technologies and Applications (FIESTA) Conference*.
- [4] P. Chendke, H. Fogler, Second-order sonochemical phenomena—extensions of previous work and applications in industrial processing, *Chem. Eng. J.* 8 (3) (1974) 165–178.
- [5] A.S. Adeleye, J.R. Conway, K. Garner, Y. Huang, Y. Su, A.A. Keller, Engineered nanomaterials for water treatment and remediation: costs, benefits, and applicability, *Chem. Eng. J.* 286 (2016) 640–662.
- [6] Y. Adewuyi, Sonochemistry: Environmental science and engineering applications, *Ind. Eng. Chem. Res.* 40 (22) (2001) 4681–4715, Cited By 471.
- [7] C. Solans, P. Izquierdo, J. Nolla, N. Azemar, M. Garcia-Celma, Nano-emulsions, *Curr Opin Colloid Interface Sci* 10 (3–4) (2005) 102–110.
- [8] M. Ashokkumar, D. Sunartio, S. Kentish, R. Mawson, L. Simons, K. Vilku, C.K. Versteeg, Modification of food ingredients by ultrasound to improve functionality: a preliminary study on a model system, *Food Sci. Emerg. Technol.* 9 (2) (2008) 155–160, *Food Innovation: Emerging Science, Technologies and Applications (FIESTA) Conference*.
- [9] K. Kezia, J. Lee, B. Zisu, M. Weeks, G. Chen, S. Gras, S. Kentish, Crystallisation of minerals from concentrated saline dairy effluent, *Water Res.* 101 (2016) 300–308, <http://dx.doi.org/10.1016/j.watres.2016.05.074>.
- [10] T.S. Leong, G.J. Martin, M. Ashokkumar, Ultrasonic encapsulation – a review, *Ultrason. Sonochem.* (2016).
- [11] T. Van Gerven, A. Stankiewicz, Structure, energy, synergy, time – The fundamentals of process intensification, *Ind. Eng. Chem. Res.* 48 (5) (2009) 2465–2474.
- [12] T. Mason, E. Cordemans, Ultrasonic intensification of chemical processing and related operations: a review, *Chem. Eng. Res. Des.* 74 (5) (1996) 511–516, Cited By 72.
- [13] P.R. Gogate, S. Mujumdar, A.B. Pandit, Large-scale sonochemical reactors for process intensification: design and experimental validation, *J. Chem. Technol. Biotechnol.* 78 (6) (2003) 685–693.
- [14] B.A. Bhanvase, D.V. Pinjari, P.R. Gogate, S.H. Sonawane, A.B. Pandit, Process intensification of encapsulation of functionalized CaCO<sub>3</sub> nanoparticles using ultrasound assisted emulsion polymerization, *Chem. Eng. Process.: Process Intensif.* 50 (12) (2011) 1160–1168.
- [15] D. Fernandez Rivas, S. Kuhn, Synergy of microfluidics and ultrasound, *Top. Curr. Chem.* 374 (5) (2016) 70.
- [16] S. Seidi, Y. Yamini, Analytical sonochemistry: developments, applications, and hyphenations of ultrasound in sample preparation and analytical techniques, *Open Chem.* 10 (4) (2012) 938–976.
- [17] K. Suslick, Sonochemistry, *Science* 247 (4949) (1990) 1439–1445.
- [18] M. Chappat, Some applications of emulsions, *Colloids Surf. A: Physicochem. Eng. Aspects* 91 (1994) 57–77.
- [19] S. Schultz, F. Wagner, K. Urban, J. Ulrich, High-pressure homogenization as a process for emulsion formation, *Chem. Eng. Technol.* 27 (4) (2004) 361–368, <http://dx.doi.org/10.1002/ceat.200406111>.
- [20] K. Schroën, O. Bliznyuk, K. Muijlwijk, S. Sahin, C. Berton-Carabin, Microfluidic emulsification devices: from micrometer insights to large-scale food emulsion production, *Curr. Opin. Food Sci.* 3 (2015) 33–40.
- [21] C.-J. Cheng, L.-Y. Chu, R. Xie, Preparation of highly monodisperse w/o emulsions with hydrophobically modified spg membranes, *J. Colloid Interface Sci.* 300 (1) (2006) 375–382.
- [22] M.L. Steegmans, K.G. Schroën, R.M. Boom, Characterization of emulsification at flat microchannel y junctions, *Langmuir* 25 (6) (2009) 3396–3401.
- [23] K. Schroën, C. Berton-Carabin, Production, Handling and Characterization of Particulate Materials, Springer International Publishing, Switzerland, 2016, *Ch. Emulsification: Established and Future Technologies*.
- [24] P. Walstra, *Physical Chemistry of Foods*, CRC Press, 2002.
- [25] T.G. Leighton, Bubble population phenomena in acoustic cavitation, *Ultrason. Sonochem.* 2 (2) (1995) S123–S136.
- [26] L.L. Hecht, T. Merkel, A. Schoth, C. Wagner, K. Köhler, R. Muñoz-Espí, K. Landfester, H.P. Schuchmann, Emulsification of particle loaded droplets with regard to miniemulsion polymerization, *Chem. Eng. J.* 229 (2013) 206–216.
- [27] J. Canselier, H. Delmas, A. Wilhelm, B. Abismail, Ultrasonic emulsification—an overview, *J. Dispersion Sci. Technol.* 23 (1–3) (2002) 333–349.
- [28] C. Jimenez-Gonzalez, P. Poechlauer, Q. Broxterman, B. Yang, D. Am Ende, J. Baird, C. Bertsch, R. Hannah, P. Dell’Orco, H. Noorman, S. Yee, R. Reintjens, A. Wells, V. Massonneau, J. Manley, Key green engineering research areas for sustainable manufacturing: a perspective from pharmaceutical and fine chemicals manufacturers, *Org. Process Res. Devel.* 15 (4) (2011) 900–911.
- [29] D. Fernandez Rivas, P. Cintas, J. Gardeniers, Merging microfluidics and sonochemistry: towards greener and more efficient micro-sono-reactors, *Chem. Commun.* 48 (89) (2012) 10935–10947.
- [30] P. Cintas, S. Tagliapietra, M. Caporaso, S. Tabasso, G. Cravotto, Enabling technologies built on a sonochemical platform: challenges and opportunities, *Ultrason. Sonochem.* 25 (1) (2015) 8–16, Cited By 2.
- [31] D. Rossi, R. Jamshidi, N. Saffari, S. Kuhn, A. Gavrilidis, L. Mazzei, Continuous-Flow Sonocrystallization in Droplet-Based Microfluidics, *Cryst. Growth Des.* (2015), <http://dx.doi.org/10.1021/acs.cgd.5b01153>.
- [32] S. Kuhn, T. Noël, L. Gu, P.L. Heider, K.F. Jensen, A Teflon microreactor with integrated piezoelectric actuator to handle solid forming reactions, *Lab Chip* 11 (15) (2011) 2488–2492.
- [33] F. Castro, S. Kuhn, K.F. Jensen, A. Ferreira, F. Rocha, A. Vicente, J.A. Teixeira, Continuous-flow precipitation of hydroxyapatite in ultrasonic microsystems, *Chem. Eng. J.* 216 (2013) 979–987.
- [34] K. Prasad, S. Sonawane, M. Zhou, M. Ashokkumar, Ultrasound assisted synthesis and characterization of poly(methyl methacrylate)/caco3 nanocomposites, *Chem. Eng. J.* 219 (2013) 254–261.
- [35] B. Bhanvase, D. Pinjari, P. Gogate, S. Sonawane, A. Pandit, Synthesis of exfoliated poly(styrene-co-methyl methacrylate)/montmorillonite nanocomposite using ultrasound assisted in situ emulsion copolymerization, *Chem. Eng. J.* 181–182 (2012) 770–778.
- [36] D. Kobayashi, H. Matsumoto, C. Kuroda, Improvement of indirect ultrasonic irradiation method for intensification of emulsion polymerization process, *Chem. Eng. J.* 135 (1–2) (2008) 43–48, *Process Intensification and Innovation – Cleaner, Sustainable, Efficient Technologies for the Future ECI Process Intensification S.I.*
- [37] T.R. Bastami, M. Entezari, Sono-synthesis of mn3o4 nanoparticles in different media without additives, *Chem. Eng. J.* 164 (1) (2010) 261–266.
- [38] B.M. Teo, S.W. Prescott, M. Ashokkumar, F. Grieser, Ultrasound initiated miniemulsion polymerization of methacrylate monomers, *Ultrason. Sonochem.* 15 (1) (2008) 89–94.
- [39] D. Fernandez Rivas, A. Prosperetti, A.G. Zijlstra, D. Lohse, J.G.E. Gardeniers, Efficient sonochemistry through microbubbles generated with micromachined surfaces, *Angew. Chem. Int. Ed.* 49 (50) (2010) 9699–9701.
- [40] B. Verhaagen, Y. Liu, A.G. Pérez, E. Castro-Hernandez, D. FernandezRivas, Scaled-up sonochemical microreactor with increased efficiency and reproducibility, *ChemistrySelect* 1 (2) (2016) 136–139.
- [41] D. Fernandez, B. Rivas, A. Verhaagen, E. Perez, R. Van Castro-Hernandez, K. Schroën, A. Zwielen, novel ultrasonic cavitation enhancer, *J. Phys.: Conf. Ser.* 656 (2015) 116–123.
- [42] J.J. John, S. Kuhn, L. Braeken, T. van Gerven, Ultrasound assisted liquid–liquid extraction in microchannels—A direct contact method, *Chem. Eng. Process.: Process Intensif.* 102 (2016) 37–46.
- [43] T. Mason, A. Cobley, J. Graves, D. Morgan, New evidence for the inverse dependence of mechanical and chemical effects on the frequency of ultrasound, *Ultrason. Sonochem.* 18 (1) (2011) 226–230.

- [44] T.J. Mason, D. Peters, 2nd ed., *Practical Sonochemistry*, Elsevier, 2002.
- [45] T. Nowak, R. Mettin, Unsteady translation and repetitive jetting of acoustic cavitation bubbles, *Phys. Rev. E.* (2014), <https://www.ncbi.nlm.nih.gov/pubmed/25314538>.
- [46] K. Schroen, M. Ferrando, S. de Lamo-Castellví, S. Sahin, C. Güell, Linking findings in microfluidics to membrane emulsification process design: the importance of wettability and component interactions with interfaces, *Membranes* 6 (2) (2016) 17–26.
- [47] V. Schröder, Herstellen von öl-in-wasser-emulsionen mit mikroporösen membranen, University of Karlsruhe (T.H.), 1999, Ph.D. thesis.
- [48] S. Sugiura, M. Nakajima, J. Tong, H. Nabetani, M. Seki, Preparation of monodispersed solid lipid microspheres using a microchannel emulsification technique, *J. Colloid Interface Sci.* 227 (2000) 95–103.
- [49] I. Kobayashi, M. Nakajima, Effect of emulsifiers on the preparation of food-grade oil-in-water emulsions using a straight-through extrusion filter, *Eur. J. Lipid Sci. Technol.* 104 (2002) 720–727.
- [50] I. Kobayashi, M. Nakajima, K. Chun, Y. Kikuchi, H. Fujita, Silicon array of elongated through-holes for monodisperse emulsion droplets, *AIChE J.* 48 (2002) 1639–1644.
- [51] K. Van Dijke, G. Veldhuis, K. Schroën, R. Boom, Parallelized edge-based droplet generation (edge) devices, *Lab Chip* 9 (2009) 2824–2830.
- [52] M. Steegmans, K. Schroën, R. Boom, Characterization of emulsification at flat microchannel y junctions, *Langmuir* 26 (6) (2009) 3396–3401.
- [53] U. Lambrich, H. Schubert, Emulsification using microporous systems, *J. Membr. Sci.* 257 (2005) 76–84.
- [54] A. Gijsbertsen-Abrahamse, A. Van Der Padt, R. Boom, Influence of membrane morphology on pore activation in membrane emulsification, *J. Membr. Sci.* 217 (2003) 141–150.
- [55] A. Gijsbertsen-Abrahamse, A. Van Der Padt, R. Boom, status of cross-flow membrane emulsification and outlook for industrial application, *J. Membr. Sci.* 230 (2004) 149–159.